Laser cooling of the alkaline-earth-metal monohydrides: Insights from an *ab initio* theory study

Yufeng Gao and Tao Gao*

Institute of Atomic and Molecular Physics, Sichuan University, Chengdu 610065, China

and Key Laboratory of High Energy Density Physics and Technology of Ministry of Education, Sichuan University, Chengdu 610065, China

(Received 4 July 2014; published 10 November 2014)

The feasibility of laser cooling MH (M = Be, Mg, Ca, Sr, and Ba) is investigated using *ab initio* quantum chemistry. The ground state $X\,^2\Sigma^+$ and first excited state $A\,^2\Pi$ of MH species are calculated using the multireference configuration interaction (MRCI) level of theory. For CaH, SrH, and BaH, the spin-orbit coupling effects are also taken into account in electronic structure calculations at the MRCI level. Calculated spectroscopic constants for ^{9}BeH, ^{24}MgH, ^{40}CaH, ^{86}SrH, and ^{138}BaH show good agreement with available theoretical and experimental results. The permanent dipole moments and transition dipole moments (TDMs) of the $X\,^2\Sigma^+$ and $A\,^2\Pi$ states of MH species are also calculated at the MRCI level of theory, and they are in good agreement with previous theoretical results. With the potential energy curves and TDMs obtained, the highly diagonally distributed Franck-Condon factors f_{00} (^{9}BeH : 0.998, ^{24}MgH : 0.954, ^{40}CaH : 0.961, ^{86}SrH : 0.978, and ^{138}BaH : 0.971) for the $A\,^2\Pi\,(v' = 0) \rightarrow X\,^2\Sigma^+\,(v = 0)$ transition are determined. Radiative lifetime calculations of the $A\,^2\Pi\,(v' = 0)$ state (^{9}BeH : 82.0 ns, ^{24}MgH : 48.6 ns, ^{40}CaH : 33.3 ns, ^{86}SrH : 33.2 ns, and ^{138}BaH: 68.6 ns) are found to be short enough for rapid laser cooling. The proposed main cycling laser drives the $X\,^2\Sigma^+\,(v = 0) \rightarrow A\,^2\Pi\,(v' = 0)$ transition at wavelength λ_{00} (^{9}BeH : 497.2 nm, ^{24}MgH : 525.5 nm, ^{40}CaH : 675.4 nm, ^{86}SrH : 740.3 nm, and ^{138}BaH : 952.6 nm). The results demonstrate the possibility of laser cooling MH species, and provide a promising theoretical reference for further theoretical and experimental research on alkaline-earth-metal monohydrides.

DOI: 10.1103/PhysRevA.90.052506 PACS number(s): 33.70.Ca, 37.10.Mn, 34.20.Cf, 31.15.vn

I. INTRODUCTION

In recent years, there has been growing interest in laser cooling of diatomic polar molecules [1–5]. Laser cooling of molecules is thought to be impractical due to their complex internal structure, which makes it difficult to keep a closed optical pumping cycle with repeated optical spontaneous emissions. However, compared with atoms, the additional types of internal motion (such as vibrational and rotational degrees of freedom) of molecules provide new features for the study and manipulation, such as anisotropic long-range dipole-dipole interaction between ultracold polar molecules and additional tunable experimental parameters (electric dipole moment) in ultracold polar molecules. The theoretical and experimental studies of cold and ultracold molecules are motivated by a variety of prospective applications [6]. So far, the transverse laser cooling of molecules has been applied to beams of SrF [2] and YO [4] and the longitudinal laser cooling of molecules has been applied to a supersonic beam of CaF molecules [5]. As early as 2004, Di Rosa presented a brief survey [7] of candidate molecules for laser cooling and identified a number of hydrides including the alkaline-earth-metal monohydrides (BeH, MgH, CaH, SrH, and BaH). As with atomic systems, molecules must meet certain criteria to be potential laser cooling candidates. The first criterion is highly diagonal Franck-Condon factors (FCFs), which describe the overlap of the vibrational wave functions for different electronic states. From a practical standpoint, highly diagonal FCFs limit the number of lasers required to keep the molecule in a closed-loop cooling cycle. A second, shorter lifetimes (i.e., high spontaneous-emission rates) are highly desirable for rapid laser cooling. A third criterion is that there are no intervening electronic states to which the upper state could radiate and terminate the cycling transition.

Very recently, polar molecules (such as RaF [8], AlH [9], AlF [9], and BeF [10]) have been theoretically investigated for laser cooling of molecules. The theoretical calculations [9] indicate FCFs of AlF are equal to 0.999 92; the excited state lifetime is extremely short at 1.8 ns. Unfortunately, the laser excitation wavelength is 227 nm for AlF and there is a low-lying triplet state $a\,^3\Pi$. The calculated FCF of BeF [10] is 0.897, and the laser excitation wavelength is ~300 nm, which is not currently accessible by diode laser.

The alkaline-earth-metal species MH (M = Be, Mg, Ca, Sr, and Ba) have been nominated as laser cooling candidates [7], which share many similar properties. They all generally have highly diagonal FCFs (0.954–0.998) and shorter radiative lifetime (generally dozens of nanoseconds), and no intervening electronic states to suppress the quasiclosed cycles of electronic transitions ($A\,^2\Pi \rightarrow X\,^2\Sigma^+$). Recently, accurate line lists for three alkaline-earth-metal molecules, BeH, MgH, and CaH, in their ground electronic states were presented by Yadin *et al.* [11]. In their study, accurate line intensities are also generated using newly computed *ab initio* dipole moment curves for three molecules using high levels of theory. More recent theoretical and experimental studies, both spectroscopic and astrophysical, are summarized in Ref. [11]. Here, we do not intend to present the long history of theoretical and experimental studies that have been conducted on the three molecular species before 2012. Only more recent studies for the alkaline-earth-metal species MH (M = Be, Mg, Ca, Sr, and Ba) are presented below.

Recently, on the *ab initio* side, electron-impact cross sections of the $v \rightarrow v'$ transitions occurring between the vibrational levels of the two $X\,^2\Sigma^+$ and $A\,^2\Pi$ electronic states

*Corresponding author: gaotao@scu.edu.cn

of the BeH molecule were calculated by Celiberto *et al.* [12]; the calculations are performed with the *R*-matrix method. The potential energy curves (PECs) and transition dipole moments (TDMs) of the $X\,^2\Sigma^+$, $A\,^2\Pi$, and $B'\,^2\Sigma^+$ states of MgH have been calculated by Mostafanejad *et al.* [13] using the multireference configuration interaction (MRCI) method with large active space and basis sets; all these calculations are performed using the GAMESS-US quantum chemistry package. The Einstein AA coefficients of rovibronic lines of the $A\,^2\Pi \rightarrow X\,^2\Sigma^+$ and $B'\,^2\Sigma^+ \rightarrow X\,^2\Sigma^+$ transitions of ^{24}MgH have been calculated by GharibNezhad *et al.* [14]. In 2013, new high-resolution visible Fourier transform emission spectra of the $A\,^2\Pi \rightarrow X\,^2\Sigma^+$ and $B'\,^2\Sigma^+ \rightarrow X\,^2\Sigma^+$ systems of ^{24}MgD and of the $B'\,^2\Sigma^+ \rightarrow X\,^2\Sigma^+$ systems of ^{25,26}MgD and ^{25,26}MgH have been combined with earlier results for ^{24}MgH in a multi-isotopologue direct-potential-fit analysis to yield improved analytic potential energy and Born-Oppenheimer breakdown functions for the ground $X\,^2\Sigma^+$ state of MgH [15]. Recently, based on the previous analysis of ^{24}MgH, molecular lines of ^{25,26}MgH have been measured and molecular constants derived by Hinkle *et al.* [16]. In 2014, the molecular beam optical Zeeman spectroscopy of the (0, 0) $A\,^2\Pi - X\,^2\Sigma^+$ band system of MgH has been reported and analyzed by Zhang *et al.* [17]. Recently, the permanent electronic dipole moments (PDMs) of MgD were obtained experimentally for $A\,^2\Pi$ ($\upsilon = 0$,2.567D) and $X\,^2\Sigma^+$ ($\upsilon = 0$, 1.31 D) by Steimle *et al.* [18]. For CaH, on the theoretical side, the Einstein A coefficients and absolute line intensities have been calculated for the $E\,^2\Pi \rightarrow X\,^2\Sigma^+$ transition by Li *et al.* [19]. On the experimental side, the emission spectra of the $A\,^2\Pi \rightarrow X\,^2\Sigma^+$ and $B\,^2\Sigma^+ \rightarrow X\,^2\Sigma^+$ transitions of CaD were produced in a discharge-furnace emission source and recorded with a high-resolution Fourier transform spectrometer by GharibNezhad *et al.* [20]. Then high-resolution Fourier transform emission spectra of CaH were obtained experimentally in the 12 000−17 000 cm^{-1} spectral region for the $A\,^2\Pi \rightarrow X\,^2\Sigma^+$ and $B\,^2\Sigma^+ \rightarrow X\,^2\Sigma^+$ transitions by Shayesteh *et al.* [21]. For SrH, on the *ab initio* side, the first four electronic states ($X\,^2\Sigma^+$, $A\,^2\Pi$, $B\,^2\Sigma^+$ and $A'^2\Delta$ states) were calculated by Leiniger *et al.* [22]; the calculations revealed a double potential regarding the $B\,^2\Sigma^+$ state. The FCFs of a few transitions of SrH and SrD have been calculated by Ramchandran *et al.* [23] due to possible astrophysical interest. On the experimental side, the lifetime of the $A\,^2\Pi$ state of SrH was measured by Berg *et al.* [24] using the method of time-resolved laser spectroscopy, and a lifetime of 33.8 ± 1.9 ns was obtained for the $\upsilon = 0$ vibrational level of the $A\,^2\Pi$ state. More recently, lifetimes of 33.2 ± 3.2 ns and 33.7 ± 5.3 ns for the $\upsilon = 0$ and 1 vibrational levels of the $A\,^2\Pi$ state and 48.4 ± 2.0 ns, and 50.5 ± 3.2 ns for the $B\,^2\Sigma^+$ state of SrH have been measured by Pauchard *et al.* [25]. In 2004, the vibration-rotation spectra of SrH and CaH were measured by Shayesteh *et al.* [26] for the $1 \rightarrow 0$ to $4 \rightarrow 3$ bands using a Fourier transform spectrometer. More recently, high-resolution spectra of the $E\,^2\Pi \rightarrow X\,^2\Sigma^+$ transiton of SrH and SrD have been obtained by Ram *et al.* [27] using a Fourier transform spectrometer. In a recent theoretical calculation on the spectroscopic properties of the ground state of all MH and MH$^+$ systems (M = Be, Mg, Ca, Sr, and Ba), Fuentealba *et al.* [28,29] have systematically studied the electronic structure of MH and MH$^+$ systems. Recently, Kaupp *et al.* [30] achieved a systematic comparison of the results obtained with two-electron+core-valence polarization pseudopotentials and ten-electron effective core potentials for MH and MH$^+$ systems (M = Ca, Sr, Ba). Then the electronic structure of BaH was determined using a ten-electron effective core potential and core-polarization potential by Allouche *et al.* [31]. More recently, the main electronic properties, PECs, PDMs, and TDMs, static dipole polarizabilities of the alkaline-earth-metal hydride ion CaH$^+$, as well as of SrH$^+$ and BaH$^+$ were computed by Aymar *et al.* [32] through a full configuration interaction (FCI) performed in a two-valence electronic configuration space build from a large Gaussian basis set. On the experimental side, radiative lifetimes of the $B\,^2\Sigma^+$ state of BaH have been measured by Berg *et al.* [33] using the laser resonance method. A lifetime of 125 ± 2 ns was obtained for the $\upsilon = 0$ vibrational level at $J = 5.5$ of the $B\,^2\Sigma^+$ state. The vibration-rotation transitions in the $X\,^2\Sigma^+$ ground electronic state have been measured by Magg *et al.* [34] and Walker *et al.* [35]. More recently, the emission spectra of the $E\,^2\Pi \rightarrow X\,^2\Sigma^+$ electronic transition of BaH have been observed by Ram *et al.* [36] at high resolution using a Fourier transform spectrometer.

As mentioned above, the alkaline-earth-metal species MH (M = Be, Mg, Ca, Sr, and Ba) have been studied extensively

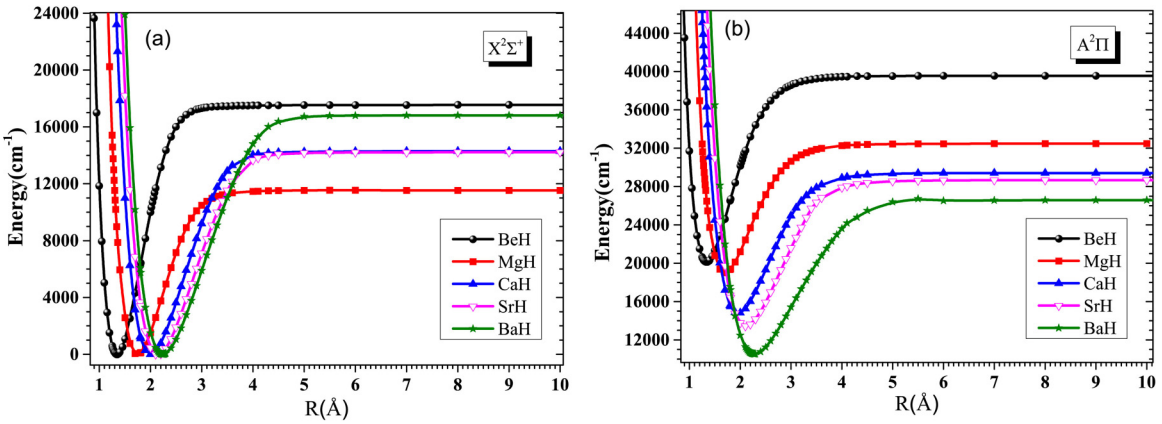

FIG. 1. (Color online) (a) PECs of $X\,^2\Sigma^+$ states and (b) $A\,^2\Pi$ states of MH (M = Be, Mg, Ca, Sr, and Ba) calculated at the MRCI level of theory.

in the past. However, there is a need for systematic, theortetical and experimental studies of laser cooling of MH (M = Be, Mg, Ca, Sr, and Ba). In this paper, thus, we would like to focus on the theoretical investigations of the electronic structures and radiative properties, mainly the FCFs and diode laser excitation wavelengths of the $A\,^2\Pi - X\,^2\Sigma^+$ electronic transition of MH species. Additionally, we briefly design a scheme for a viable laser cooling cycle for MH species.

The paper is organized as follows. In Sec. II, we describe the theoretical methods and basis sets used in the *ab initio*

TABLE I. Spectroscopic constants for $X\,^2\Sigma^+$ and $A\,^2\Pi$ states of MH (M = Be, Mg, Ca, Sr, and Ba) at MRCI level.

Molecule	States	T_e(cm^{-1})	R_e(Å)	ω_e(cm^{-1})	$\omega_e\chi_e$(cm^{-1})	B_e(cm^{-1})	D_e(eV)	Reference
^{9}Be^{1}H	$X\,^2\Sigma^+$		1.3464	2168.29	55.426	10.260	2.175	This work
			1.346	2081	57.4	10.266	2.12	Ref. [53]
			1.316	2128.55	44.924	10.730	2.245	Ref. [54]
			1.3426	2060.78	36.310	10.316	2.181	Exp.[a]
	$A\,^2\Pi$	20 123.9	1.3380	2136.02	51.903	10.390	2.409	This work
		20 244.5	1.338	2074	39.7	10.374	2.36	Ref. [53]
		20 055.8	1.309	2155.5	47.769	10.847	2.79	Ref. [54]
		20 033.2	1.3336	2088.58	40.140	10.457	2.404	Exp.[a]
^{24}Mg^{1}H	$X\,^2\Sigma^+$		1.742	1643.2	53.1	5.743	1.429	This work
			1.741	1491.6	31.0		1.427	Ref. [13]
			1.72	1453.7	29.4		1.361	Ref. [60]
			1.741	1485.6	28.9		1.434	Ref. [56]
			1.730	1492.8	29.8		1.377	Exp.[b]
	$A\,^2\Pi$	19 001.4	1.696	1646.5	45.54	6.061	1.677	This work
		18 924	1.693	1581.5	34.4		1.676	Ref. [13]
		19 397	1.67	1551.3	31.2		1.643	Ref. [60]
		18 893	1.693	1580.8	30.2		1.6875	Ref. [56]
		19 225.5	1.678	1600.3	31.87		1.705	Exp.[b]
^{40}Ca^{1}H	$X\,^2\Sigma^+$		2.0014	1308.23	21.1	4.281	1.772	This work
			1.99	1284			1.699	Ref. [61]
			2.0025	1298.34	19.1	4.2766	1.837	Exp.[a]
				1298.40	19.2	4.2770		Exp.[c]
	$A\,^2\Pi$	14 778.6	1.9562	1403.33	26.0	4.4813	1.815	This work
		14 524	1.97	1326			1.784	Ref. [61]
		14 413	1.9740	1333	20	4.3477	1.883	Exp.[a]
		14 406.9	1.9821	1336.3	20.2	4.3648		Exp.[c]
^{86}Sr^{1}H	$X\,^2\Sigma^+$		2.1430	1222.88	18.4	3.6848	1.768	This work
			2.21	1167	19	3.43	1.47	Ref. [22]
			2.211	1166.2		3.45		Ref. [62]
			2.1456	1206.2	17.0	3.6751		Exp.[a]
			2.1461	1207.0	17.2	3.6735		Exp.[d]
	$A\,^2\Pi$	13 487.3	2.1090	1273.03	17.7	3.8046	1.887	This work
		13 571	2.16	1175	14	3.52	1.75	Ref. [22]
		13 112	2.172	1214.5		3.58		Ref. [62]
		13 500	2.121	1253.9	18.0	3.72		Ref. [63]
			2.148			3.668		Exp.[a]
^{138}Ba^{1}H	$X\,^2\Sigma^+$		2.2417	1159.88	14.22	3.3527	2.08	This work
			2.262	1196	16.3	3.294	1.97	Ref. [31]
			2.2319	1168.43	14.61	3.3825	<1.95	Exp.[e]
			2.2319	1168.43	14.61	3.3824		Exp.[f]
	$A\,^2\Pi$	10 630.1	2.2821	1108.44	15.20	3.2350	2.01	This work
		9872	2.293	1136	16.7	3.205		Ref. [31]
		9700	2.2735	1115.9	16.5	3.2597		Exp.[g]

[a]Reference [55].
[b]References [57–59].
[c]Reference [21].
[d]Reference [26].
[e]Reference [34].
[f]Reference [36].
[g]Reference [64].

calculations for the lowest two electronic states ($X\,^2\Sigma^+$ and $A\,^2\Pi$) of MH species. Section III shows the results and a discussion of the data, outlining laser cooling schemes for MH species. In Sec. IV, we give a conclusion for this work.

II. METHOD

In the present work, the *ab initio* electronic structure calculations for the two lowest doublet electronic states ($X\,^2\Sigma^+$ and $A\,^2\Pi$) of the MH (M = Be, Mg, Ca, Sr, and Ba) species have been performed with complete active space self-consistent field (CASSCF) [37,38] and MRCI plus Davidson corrections (MRCI+Q) [39–41] methods. Scalar relativistic effects were accounted for using the Douglas-Kroll-Hess (DHK) [42,43] transformation of the relativistic Hamiltonian. For CaH, SrH, and BaH, the spin-orbit coupling effects are also taken into account in electronic structure calculations at the MRCI level. All the *ab initio* calculations are carried out in the C_{2v} symmetry using the MOLPRO package [44].

In CASSCF and subsequent MRCI calculations of BeH and MgH, the basis sets aug-cc-PVQZ-DK [45,46] were used for Be and Mg, aug-cc-PV5Z [47] for H, and all the core electrons below Be($1s$) and Mg($2p$) are frozen and hence the excitations are taken to be from H $1s$, Be $2s$, and Mg $3s$ orbitals. For Ca, Sr, and Ba, we use the small-core scalar relativistic effective core potential (ECP) ECP10MDF [48], ECP28MDF [48], and ECP46MDF [48] together with the corresponding valence basis sets [48], respectively. In C_{2v} point group, all molecular orbitals were labeled by their symmetry (a_1,b_1,b_2,a_2); when symmetry is reduced from $C_{2\infty}$ to C_{2v}, the correlating relationships are $\sigma \rightarrow a_1, \pi \rightarrow (b_1,b_2), \delta \rightarrow (a_1,a_2)$. The active space consists of three electrons and thirteen molecular orbitals $7a_1$, $3b_1$, $3b_2$, $0a_2$ (7330) which correspond with the Be $2s2p3s3p3d$ and H $1s$ and is referred to as CAS (3, 13); the d_{xy} component was removed from the active space. For MgH, a larger active space (7331) was determined in the same way with the calculations of BeH, which is referred to as CAS (3, 14). For CaH, SrH, and BaH, these active spaces are (3110), (4110), and (4111), respectively. The eight electrons in the Ca $3s3p$, Sr $4s4p$, and Ba $5s5p$ shells were put in the closed spaces, respectively. These closed spaces were doubly occupied in all reference configuration state functions, but were still optimized.

For heavier elements, spin-orbit coupling (SOC) becomes important for the electronic structure. An additional effect of a large splitting of the electron energy levels results from the SOC. Thus in our calculations, SOC effects were also taken into account for CaH, SrH, and BaH with the SOC operator H_{SO} defined within the Breit-Pauli approximation [49] at the MRCI level of theory. All-electron basis sets CVTZ [50], DZP-DKH [51] were used in the calculations of Ca and Sr, respectively. In order to mimic the scalar relativistic effects some electrons were described by pseudopotentials. For Ba we took the ECP46MDF [48] pseudopotentials and *spdfg* quality basis set suggested in Ref. [48] from the Stuttgart library. The augmented cc-pV5Z (AV5Z) basis set is used for H. We performed CASSCF and MRCI calculations with active spaces consisting of Ca $3s3p4s4p$, Sr $4s4p5s5p$, Ba $6s5d$, and H $1s$, respectively.

We evaluated equilibrium bond distance (R_e), dissociation energy (D_e), harmonic frequency (ω_e), anharmonic vibrational frequency ($\omega_e\chi_e$), rotational constant (B_e), and electronic transition energy (T_e) for the $X\,^2\Sigma^+$ and $A\,^2\Pi$ states of the MH (M = Be, Mg, Ca, Sr, and Ba) species using Le Roy's LEVEL8.0 program [52]. We also present PDMs and TDMs of MH species computed by taking the expectation and transition values using the MRCI wave functions.

III. RESULTS

A. Potential energy curves and spectroscopic constants of $X\,^2\Sigma^+$ and $A\,^2\Pi$ states of MH (M = Be, Mg, Ca, Sr, and Ba)

1. Results without spin-orbit coupling

In Figs. 1(a) and 1(b), we present the PECs of $X\,^2\Sigma^+$ and $A\,^2\Pi$ states of MH (M = Be, Mg, Ca, Sr, and Ba) species at the MRCI level of theory, respectively. The corresponding spectroscopic constants are tabulated in Table I. Because our main interest is in the first two electronic states that are relevant for laser cooling, we have restricted our calculations to the two states ($X\,^2\Sigma^+$ and $A\,^2\Pi$) only. In order to estimate the accuracy of our PECs and the spectroscopic constants, we compared our results with available theoretical and experimental values which are also listed in Table I together. For BeH, the spectroscopic constants calculated at MRCI level compare very well with the available (Configuration Interaction

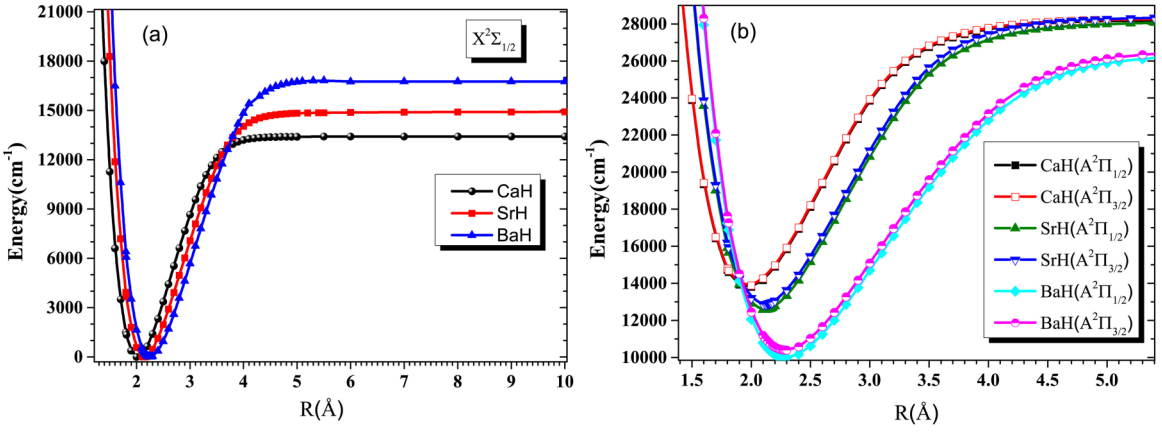

FIG. 2. (Color online) (a) PECs of $X\,^2\Sigma_{1/2}$ states and (b) $A\,^2\Pi_{1/2,3/2}$ states of MH (M = Ca, Sr, Ba) calculated at the MRCI level of theory.

TABLE II. Spectroscopic constants for $X\,^2\Sigma_{1/2}$ and $A\,^2\Pi_{1/2,3/2}$ states of MH (M = Ca, Sr, Ba) at MRCI level including spin-orbit coupling.

Molecule	Ω states	T_e(cm^{-1})	R_e (Å)	ω_e(cm^{-1})	$\omega_e\chi_e$(cm^{-1})	B_e(cm^{-1})	D_e (eV)	Reference
^{40}Ca^{1}H	$X\,^2\Sigma_{1/2}$	0	2.0183	1301.81	23.15	4.2024	1.6642	This work
		0	2.0025	1298.34	19.10	4.2766		Exp.[a]
	$A\,^2\Pi_{1/2}$	13 796.55	1.9702	1392.22	25.41	4.4131	1.7908	This work
		14 413	1.9740	1333	20	4.3477		Exp.[a]
	$A\,^2\Pi_{3/2}$	13 871.31	1.9700	1392.89	25.46	4.4139	1.7895	This work
		14 413	1.9740	1333	20	4.3477		Exp.[a]
^{86}Sr^{1}H	$X\,^2\Sigma_{1/2}$	0	2.1458	1232.56	19.08	3.6753	1.8486	This work
		0	2.1456	1206.2	17.0	3.6751		Exp.[a]
	$A\,^2\Pi_{1/2}$	12 569.38	2.1092	1309.81	20.60	3.8052	1.9315	This work
		13 571	2.16	1175	14	3.52	1.75	Ref [22].
	$A\,^2\Pi_{3/2}$	12 871.04	2.1086	1311.08	20.58	3.8074	1.9275	This work
		13 804	2.16	1173	13	3.57	1.76	Ref [22].
^{138}Ba^{1}H	$X\,^2\Sigma_{1/2}$	0	2.2552	1147.77	13.76	3.3127	2.0860	This work
		0	2.23175	1168.31	14.50	3.382 85		Exp.[a]
	$A\,^2\Pi_{1/2}$	9988.66	2.2925	1096.92	14.95	3.2057	2.0118	This work
		9457.45	2.249	1110.55	15.29	3.278 87		Exp.[a]
	$A\,^2\Pi_{3/2}$	10 398.17	2.2918	1096.43	15.04	3.2078	1.9877	This work
		9939.82	2.249	1109.98	13.59	3.322		Exp.[a]

[a]Reference [55].

with Single, Double, and Triple Excitations) CISDT [53] calculations (for $X\,^2\Sigma^+$, $R_e \sim 0.0004$ Å, $\omega_e \sim 87.29$ cm^{-1}, $\omega_e\chi_e \sim 1.97$ cm^{-1}, $B_e \sim 0.006$ cm^{-1}, $D_e \sim 0.055$ eV; for $A\,^2\Pi$, $R_e \sim 0.000$ Å, $\omega_e \sim 62.02$ cm^{-1}, $\omega_e\chi_e \sim 12.20$ cm^{-1}, $B_e \sim 0.016$ cm^{-1}, $D_e \sim 0.049$ eV). At the same time, full configuration interaction (FCI) calculations by Pitarch-Ruiz *et al.* [54] yield a shorter bond length (∼0.0304 Å, ∼0.029 Å, for $X\,^2\Sigma^+$ and $A\,^2\Pi$, respectively). Comparing our results with experimental values [55], R_e and D_e are shown to be accurate to better than 0.33% for $X\,^2\Sigma^+$ and $A\,^2\Pi$ states of BeH. For MgH, calculations for D_e of $X\,^2\Sigma^+$ state by Mostafanejad *et al.* [13] and Guitou *et al.* [56], including our MRCI results, are found to be overestimated (∼0.05 eV) with respect to experiment [57–59], except for Ref. [60]. And for $A\,^2\Pi$ state of MgH, the calculated D_e [13,56,60] were all underestimated (∼0.029, 0.062, and 0.0175 eV) with respect to experiment 1.705 eV [57–59]. For CaH, good agreement is found for our results; in Leininger *et al.* [61] and the recent experiment values [21,55], for example, the errors of R_e and D_e are within 0.9% and 3.6%, respectively. In a recent theoretical calculation on the $X\,^2\Sigma^+$ and $A\,^2\Pi$ states of SrH, a larger R_e (∼0.064/0.0654 Å, ∼ 0.012/0.024 Å) with respect to experiment (2.1456/2.1461 Å, 2.148 Å) [26,55] have been estimated by Leininger *et al.* [22] and Korek *et al.* [62]. Shorter bond lengths (∼ 0.027 Å/0.039 Å) for the $A\,^2\Pi$ state of SrH have been obtained by Appelblad *et al.* [63] and our present work. For BaH, a very good agreement can be found for our results, Allouche *et al.* [31], and recent experiment values [64]. The $X\,^2\Sigma^+$ and $A\,^2\Pi$ states have equilibrium bond lengths of 2.2417 and 2.2821 Å, respectively, while the corresponding experimental values are 2.2319 and 2.2735 Å, and the relative errors are only 0.44% and 0. 86%, respectively.

The results show that the theoretical and experimental data agree well.

2. *Results including spin-orbit coupling for* CaH, SrH, *and* BaH

The spin-orbit PECs of CaH, SrH, and BaH are shown in Figs. 2(a) ($X\,^2\Sigma_{1/2}$) and 2(b) ($A\,^2\Pi_{1/2,3/2}$), with their

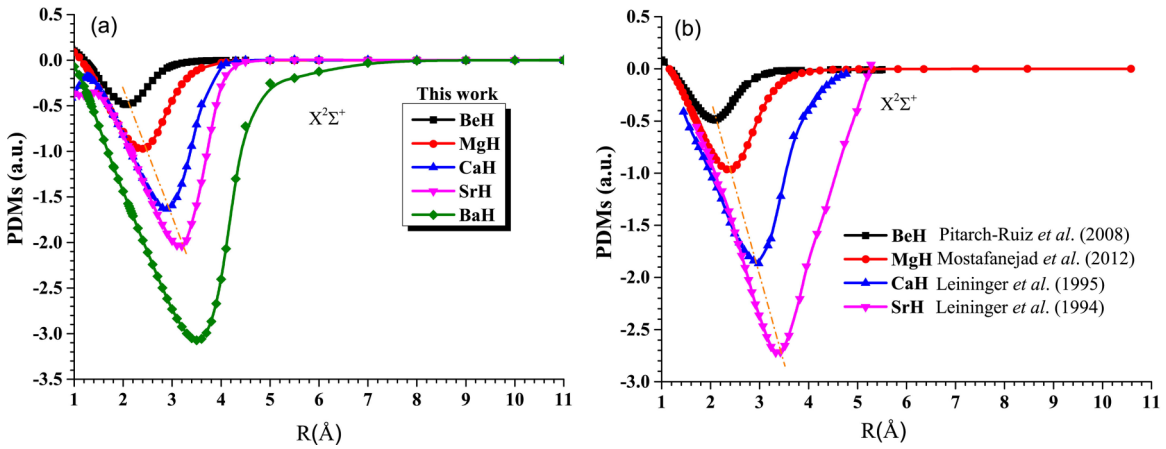

FIG. 3. (Color online) (a) PDMs of ground $X\,^2\Sigma^+$ state at MRCI level for MH species; (b) The other theoretical PDMs of $X\,^2\Sigma^+$ state for MH (M = Be, Mg, Ca, Sr).

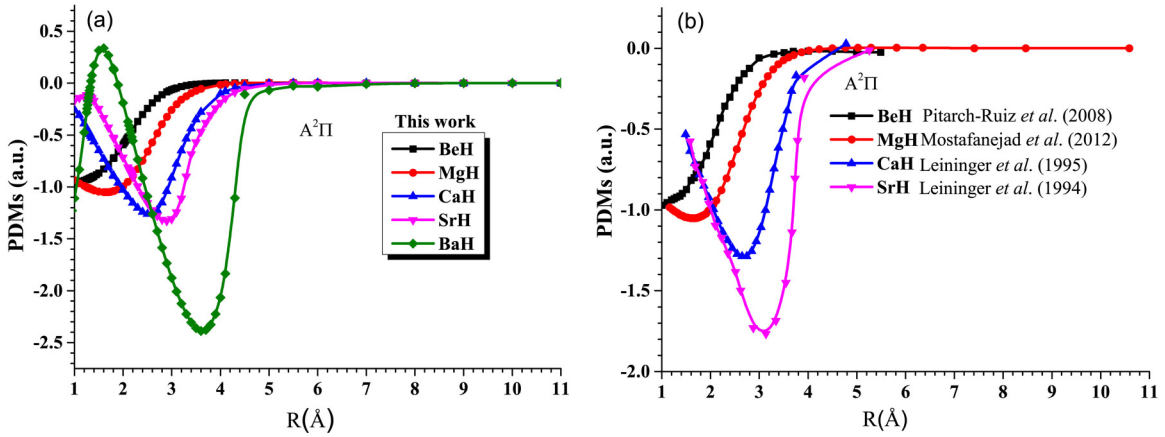

FIG. 4. (Color online) (a) PDMs of excited $A\,^2\Pi$ state at MRCI level for MH species. (b) The other theoretical PDMs of $A\,^2\Pi$ state for MH (M = Be, Mg, Ca, Sr).

corresponding spectroscopic constants in Table II. The ground molecular states $X\,^2\Sigma_{1/2}$ dissociate to ground H($^2S_{1/2}$) and ground Ca($^1S_0$), Sr($^1S_0$), and Ba($^1S_0$) atomic asymptotes, respectively. The excited states $A\,^2\Pi_{1/2,3/2}$ dissociate to excited Ca($^3P_{0,1}$), Sr($^3P_{0,1}$), and Ba($^3D_1$) states, respectively.

Examining carefully the spectroscopic constants without (Table I) and with the SOC (Table II) of CaH, SrH, and BaH, we can find that the main differences with spectroscopic constants of ΛS states concern T_e, which is a direct consequence of the splitting for Ω states related to $A\,^2\Pi$ parents. The influence of spin-orbit coupling on other spectroscopic properties is generally weaker. The properties of $X\,^2\Sigma_{1/2}$ ground states are almost identical to those of their $X\,^2\Sigma^+$ parents, and the variations are very small ($\delta R_e = 0.0028-0.0169$ Å, $\delta\omega_e = 6.42-12.11$ cm^{-1}, $\delta\omega_e\chi_e = 0.46-0.05$ cm^{-1}). In the case of $A\,^2\Pi_{1/2,3/2}$ states, the spectroscopic constants for R_e, ω_e, and $\omega_e\chi_e$ generally show only small deviations with respect to their $A\,^2\Pi$ parent states ($\delta R_e = 0.0002-0.0140$ Å, $\delta\omega_e = 11.11-36.78$ cm^{-1}, $\delta\omega_e\chi_e = 0.25-2.90$ cm^{-1} for $A\,^2\Pi_{1/2}$, and $\delta R_e = 0.0004-0.0138$ Å, $\delta\omega_e = 10.44-38.05$ cm^{-1}, $\delta\omega_e\chi_e = 0.16-2.88$ cm^{-1} for $A\,^2\Pi_{3/2}$).

These results suggest that the effect of spin-orbit coupling on the spectroscopic parameters with all-electron calculations did not show a significant impact with respect to the results of spin-free relativistic ECP-MRCI approach.

B. PDMs and TDMs of $X\,^2\Sigma^+$ and $A\,^2\Pi$ states of MH (M = Be, Mg, Ca, Sr, and Ba)

In Figs. 3(a) and 4(a), the PDMs of the $X\,^2\Sigma^+$ and $A\,^2\Pi$ states of MH (M = Be, Mg, Ca, Sr, and Ba) are plotted against the internuclear distance R at the MRCI level of theory, respectively. As shown in Fig. 3(a), the PDM functions of $X\,^2\Sigma^+$ state of MH species demonstrate similar behavior with respect to internuclear distance R, wherein the absolute magnitude gradually increases as R decreases, reaches a maximum (BeH:–0.49 a.u., MgH:–0.97 a.u., CaH:–1.63 a.u., SrH:–2.04 a.u., and BaH:–3.07 a.u.) at $R > R_e$, and drops thereafter. At the same time, we found a linear change of the absolute maximum for the PDMs of the $X\,^2\Sigma^+$ of MH (M = Be, Mg, Ca, Sr) species. For comparing, the available theoretical calculations [13,22,54,61] for the PDMs of MH (M = Be, Mg, Ca, Sr) were also illustrated in Fig. 3(b). These curves [Figs. 3(a) and 3(b)] are nearly identical, which implies that our results that rely on MRCI calculations are appropriate and reliable. For the PDMs of excited $A\,^2\Pi$ state (Fig. 4), the linear change of the absolute maximum did not exhibit clearly.

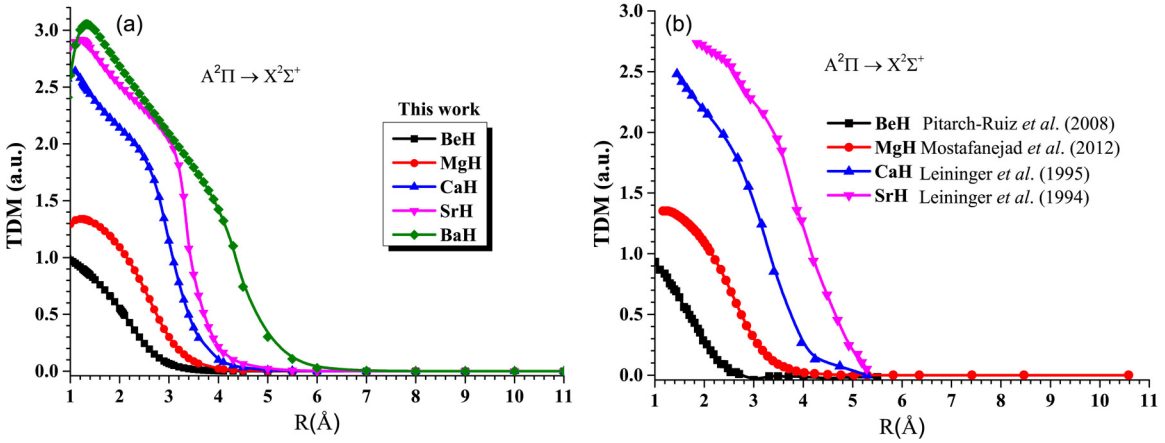

FIG. 5. (Color online) (a) TDMs computed at the MRCI level by the present work. (b) The other theoretical TDMs for $A\,^2\Pi \rightarrow X\,^2\Sigma^+$ transitions of MH (M = Be, Mg, Ca, Sr).

The relative size (BeH:–0.99 a.u., MgH:–1.05 a.u., CaH:–1.26 a.u., SrH:–1.33 a.u., and BaH:–2.39 a.u.) is consistent for the PDMs of the $X\,^2\Sigma^+$ and $A\,^2\Pi$ states of MH (M = Be, Mg, Ca, Sr, and Ba). Comparing Figs. 4(a) and 4(b), the shape difference between the present work and the other theoretical value [22] for the PDMs of $A\,^2\Pi$ of SrH is slight,

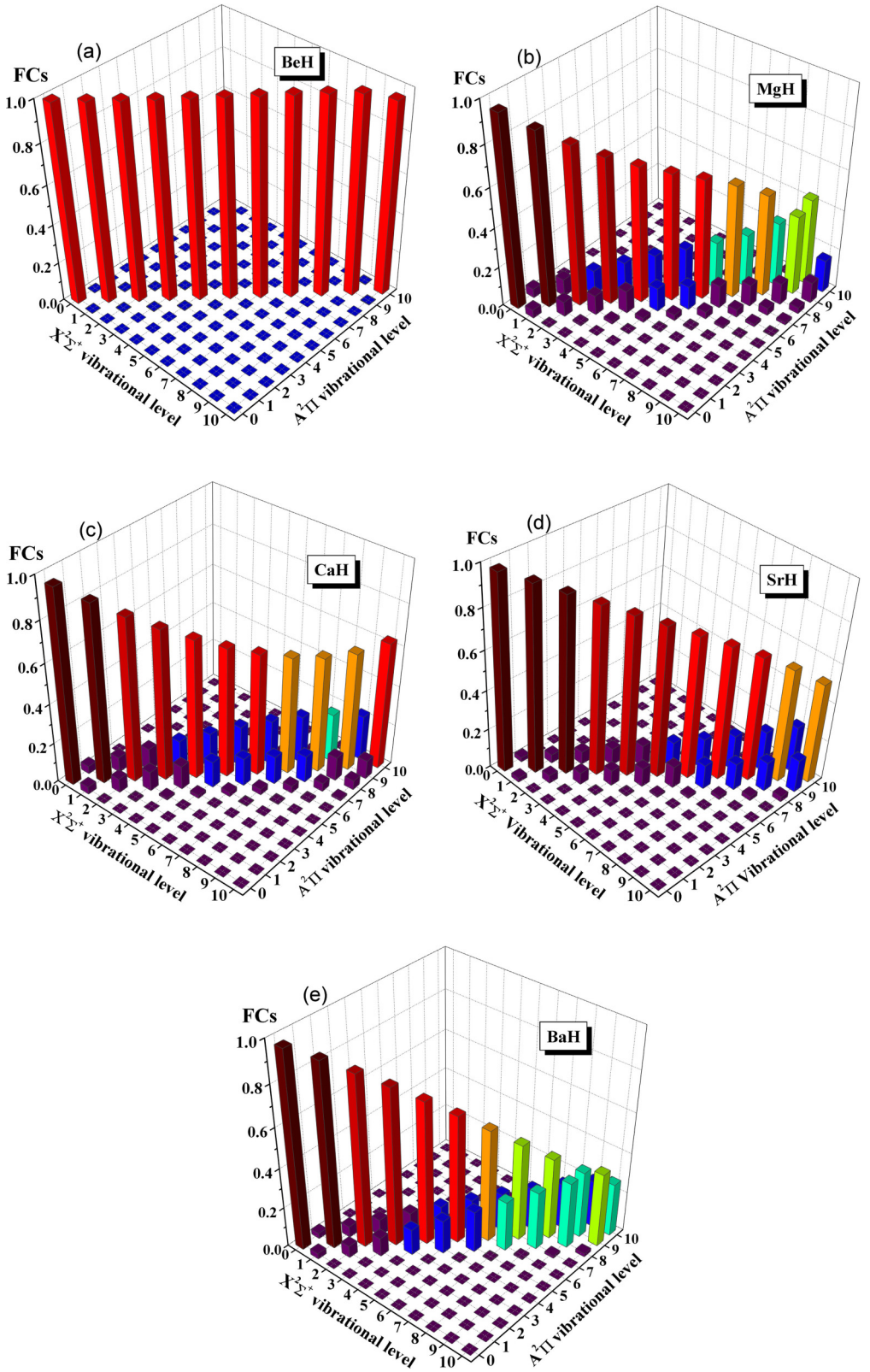

FIG. 6. (Color online) (a) BeH, (b) MgH, (c) CaH, (d) SrH, (e) BaH calculated Franck-Condon factors (FCFs) in MH (M = Be, Mg, Ca, Sr, and Ba) species for the lowest ten vibrational levels of the cooling transition $A\,^2\Pi \rightarrow X\,^2\Sigma^+$ transitions.

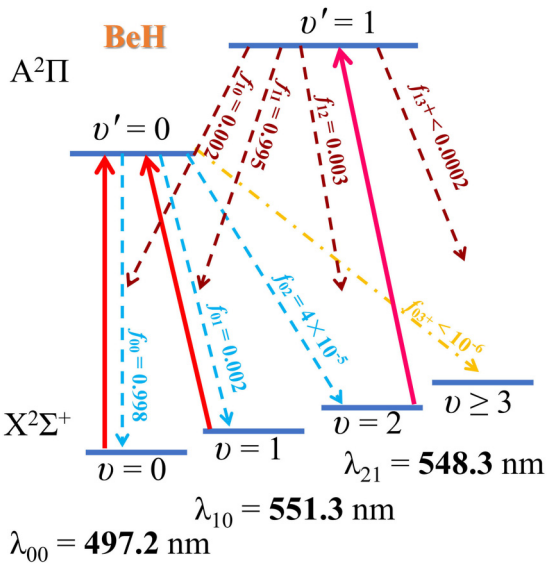

FIG. 7. (Color online) Proposed laser cooling scheme for BeH using the $X\,^2\Sigma^+ \rightarrow A\,^2\Pi$ transition (solid red and pink) and spontaneous decay (dotted line) with calculated $f_{v'v}$ for BeH molecule. Here $\lambda_{vv'}$ is the wavelength of the $X\,^2\Sigma^+(v) \rightarrow A\,^2\Pi(v')$ transition.

which can be attributed to the different basis sets [22,48] and active space used in calculations.

The TMDs between the $X\,^2\Sigma^+$ and $A\,^2\Pi$ states of MH (M = Be, Mg, Ca, Sr, and Ba) for the present work and other theoretical results are shown in Figs. 5(a) and 5(b), respectively. Like PDMs, the TDMs also demonstrate similar behavior with respect to internuclear distance R, wherein the magnitude gradually increases as R decreases, reaches a maximum (BeH: 1.01 a.u., MgH: 1.34 a.u., CaH: 2.64 a.u., SrH: 2.92 a.u., and BaH: 3.05 a.u.) at $R < R_e$, and drops thereafter. The TDMs trend to zero at large distances due to spin forbidden transitions at atomic limits from $M(^1S)$ to $M(^3P)$. Within the calculational error, our calculations give very similar shape compared with those in Ref. [13,22,54,61] in most bond length regions, but in detail the bond length dependence of the functions is different.

C. Franck-Condon overlap of the vibrational levels of $X\,^2\Sigma^+$ and $A\,^2\Pi$ states of MH (M = Be, Mg, Ca, Sr, and Ba)

The FCFs of spontaneous radiative transitions, $f_{v'v}$, are drawn in Figs. 6(a)–6(e), which describe the overlap of the vibrational wave functions for $A\,^2\Pi\ (v') \rightarrow X\,^2\Sigma^+(v)$ transition. All possible transitions between $0 \leqslant v' \leqslant 10$ and $0 \leqslant v \leqslant 10$ appear in these figures. In the present work, the FCFs for $A\,^2\Pi \rightarrow X\,^2\Sigma^+$ transition of MH all have a common feature: the $\Delta v \equiv v' - v = 0$ transitions (diagonal) have the largest probabilities of transition whereas the off-diagonal terms have very small values. This is the first criterion to be considered for candidates for laser cooling, which acknowledges the convenience if not the practical necessity of limiting the number of lasers required to keep the molecule in a closed-loop cooling cycle. Figure 7 shows the proposed laser-driven transitions (solid red and pink) and spontaneous decay (dotted line) with calculated $f_{v'v}$ for BeH molecule. The calculated f_{00} of 0.998 for BeH is larger than that predicted in SrF ($f_{00} = 0.98$); thus it is sufficiently large to be potentially viable for cooling. The main cycling laser drives the $X\,^2\Sigma^+(v = 0) \rightarrow A\,^2\Pi(v' = 0)$ transition at wavelength $\lambda_{00} = 497.2$ nm; the corresponding experimental value [65] is 499.2 nm. (Here $\lambda_{vv'}$ is the wavelength of the $X\,^2\Sigma^+(v) \rightarrow A\,^2\Pi(v')$ transition). However, there is a small probability of decay to the $X\,^2\Sigma^+(v = 1)$ state (≈0.2%) and an even smaller probability of decay to the $X\,^2\Sigma^+(v = 2)$ state (≈0.004%). Decays to the $X\,^2\Sigma^+(v \geqslant 3)$ state from the $A\,^2\Pi$ state occur with probability $\approx 10^{-6}$. As shown in Fig. 7, the branching to $v \geqslant 3$ states is $f_{03^+} < 10^{-6}$, thus using the $X\,^2\Sigma^+(v = 1) \rightarrow A\,^2\Pi(v' = 0)$ as the first vibrational repump, and the $X\,^2\Sigma^+(v = 2) \rightarrow A\,^2\Pi(v' = 1)$ transition for the second vibrational repump should result in $N_{\text{scat}} = 1/f_{03^+} > 10^6$ photons scattered before higher vibrational levels are populated. With this scheme, only three cooling lasers (one main pump laser, with $\lambda_{00} = 497.2$ nm, and two vibrational repump lasers, with $\lambda_{10} = 551.3$ nm and

TABLE III. The calculated Franck-Condon factors (FCFs) $f_{v'v}$ and wavelength $\lambda_{vv'}$ of the $X\,^2\Sigma^+(v) \rightarrow A\,^2\Pi\ (v')$ transition (experimental values in brackets). Numbers in parentheses indicate the power of 10.

Molecules	f_{00} / f_{10}	f_{01} / f_{11}	f_{02} / f_{12}	f_{03} / f_{13}	λ_{00}(nm)	λ_{10}(nm)	λ_{21}(nm)
BeH	**0.998**	0.002	3.8(–5)	1.8(–7)	497.2	551.3	548.3
	0.002	**0.995**	0.003	1.2(–4)	[499.2][a]	[554.2][a]	
MgH	**0.954**	0.042	0.003	2.4(–4)	525.5	568.1	563.6
	0.046	**0.870**	0.075	0.008	[518.7][b]	[562.3][b]	
CaH	**0.961**	0.038	0.002	1.0(–4)	675.4	738.0	732.0
	0.039	**0.885**	0.070	0.005	[693.0][c]	[759.3][c]	
SrH	**0.978**	0.021	6.0(–4)	1.5(–5)	740.3	811.1	805.0
	0.022	**0.935**	0.041	0.002	[739.4][d]	[815.0][d]	
BaH	**0.971**	0.029	7.0(–5)	4.9(–7)	952.6	1067.7	1070.3
	0.028	**0.913**	0.060	2.8(–4)	[1034][b]	[1176][b]	

[a]Reference [65].
[b]Reference [55].
[c]Reference [66].
[d]Reference [63].

TABLE IV. Estimated spontaneous radiative lifetimes (ns) and radiative width (cm^{-1}) (in italics) of the transitions from the $A\,^2\Pi$ state in the lower vibrational levels to the ground state $X\,^2\Sigma^+$ of MH (M = Be, Mg, Ca, Sr, and Ba). Numbers in parentheses following an entry are powers of 10.

Molecule	$v'=0$	1	2	3	4	5
BeH	82.0	85.4	89.3	94.0	99.8	107
	(81)[a]	(84)[a]	(88)[a]	(92)[a]	(98)[a]	(106)[a]
	6.46(–5)	*6.21(–5)*	*5.94(–5)*	*5.64(–5)*	*5.31(–5)*	*4.95(–5)*
MgH	48.6 (46.0)[b]	50.2 (47.3)[b]	52.3 (49.0)[b]	54.9	58.4	63.0
	[43.6 ± 3][c]	[44.4 ± 4][c]	–	–	–	–
	10.91(–5)	*10.56(–5)*	*10.13(–5)*	*9.65(–5)*	*9.08(–5)*	*8.41(–5)*
CaH	33.3	33.4	33.8	34.3	35.0	36.1
	[33.2 ± 3.2][d]	[33.7 ± 5.2][d]	–	–	–	–
	1.59(–4)	*1.585(–4)*	*1.57(–4)*	*1.55(–4)*	*1.51(–4)*	*1.47(–4)*
SrH	33.2	33.3	33.4	33.6	33.8	34.1
	[33.8 ± 1.9][e]	–	–	–	–	–
	1.60(–4)	*1.59(–4)*	*1.59(–4)*	*1.58(–4)*	*1.57(–4)*	*1.56(–4)*
BaH	68.6	70.5	72.5	74.6	76.9	79.4
	7.72(–5)	*7.52(–5)*	*7.31(–5)*	*7.10(–5)*	*6.89(–5)*	*6.68(–5)*

Notes: Experimental values in brackets, and theoretical values in parentheses.
[a]Reference [68].
[b]Reference [13].
[c]Reference [69].
[d]Reference [70].
[e]Reference [24].

$\lambda_{21} = 548.3$ nm) are required, as shown in Fig. 7. In order to avoid or reduce cumbersome problems, here we only show the case of BeH; other proposed laser-driven transitions and spontaneous decay data of molecules will be tabulated in Table III. While CaH [66], SrH, and BaH require diode laser excitation wavelengths in the red or IR, BeH has $\lambda_{00} \sim 500$ nm and MgH has $\lambda_{00} \sim 520$ nm. Laser diodes at 520 nm became available in 2012. The complete list of FCFs and wavelength $\lambda_{vv'}$ between $A\,^2\Pi_{1/2,3/2}(v')$ and $X\,^2\Sigma_{1/2}(v)$ states of CaH, SrH, and BaH are in the Supplemental Material [67].

D. Spontaneous radiative lifetime and radiative width for the vibrational levels of the $A\,^2\Pi$ state of MH (M = Be, Mg, Ca, Sr, Ba)

Large FCFs, however, are not enough to ensure a good laser cooling candidate, when the rate of optical cycling must also be significant (10^5–$10^8\,s^{-1}$) to produce larger spontaneous scattering forces. The second criterion is sufficiently short lifetimes, which are highly desirable for rapid laser cooling, because they could provide a significant rate of optical cycling. The spontaneous radiative lifetimes and radiative width are collected in Table IV for selected vibrational states of the transitions from the $A\,^2\Pi$ state in the lower vibrational levels to the ground state $X\,^2\Sigma^+$ of MH (M = Be, Mg, Ca, Sr, and Ba). The other available theoretical [13,68] and experimental [24,69,70] results are also presented in Table IV for comparing. For the sake of clarity, we will use both theoretical value (when available, in parentheses) and experimental value (when available, in brackets) notations for radiative lifetimes of the $A\,^2\Pi$ (v') vibrational states of the MH species. In order to illustrate them, we chose the BeH molecule as being representative of MH species (see Table IV). The radiative lifetimes of the $A\,^2\Pi$ (v') vibrational states are computed to be 82.0–107 ns for the first six vibrational levels ($v' = 0$–5) of BeH, which is in fairly good agreement with calculations of Machado *et al.* [68]. These short lifetimes are sufficient to produce large spontaneous scattering forces. At the same time, the radiative width of the $A\,^2\Pi$ (v') vibrational states are predicted to be 4.95×10^{-5} cm^{-1}–6.46×10^{-5} cm^{-1} for the first six vibrational levels ($v' = 0 - 5$) of BeH. More detailed data can be found in Table IV. As shown in Table IV, our computed radiative lifetimes are in fair agreement with the available theoretical [13,68] and experimental values [24,69,70]. The radiative lifetimes show a slight increase with increasing v' (BeH: 82.0–107 ns, MgH: 48.6–63.0 ns, CaH: 33.3–36.1 ns, SrH: 33.2–34.1 ns, and BaH: 68.6–79.4 ns). The radiative widths show a slight decrease with increasing v' (BeH : 6.46×10^{-5} cm^{-1}–4.95×10^{-5} cm^{-1}, MgH : 10.91×10^{-5} cm^{-1}–8.41×10^{-5} cm^{-1}, CaH: 1.59×10^{-4} cm^{-1}–1.47×10^{-4} cm^{-1}, SrH: 1.60×10^{-4} cm^{-1}–1.56×10^{-4} cm^{-1}, and BaH: 7.72×10^{-5} cm^{-1}–6.68×10^{-5} cm^{-1}). For CaH, SrH, and BaH, the radiative lifetimes and radiative widths of the $A\,^2\Pi_{1/2,3/2}(v')$ states can be found in the Supplemental Material [67].

IV. CONCLUSION

In the present work, *ab initio* PECs, PDMs, and TDMs have been calculated for the $X\,^2\Sigma^+$ and $A\,^2\Pi$ states of the MH (M = Be, Mg, Ca, Sr, and Ba) at the CASSCF/MRCI+Q level of theory. The aug-cc-PVQZ-DK basis set (Be, Mg), pseudopotentials ECPnDF (n = 10, 28, 46) (Ca, Sr, and Ba) and corresponding basis sets were used in the present calculations. The spectroscopic constants (T_e, R_e, D_e, ω_e, $\omega_e\chi_e$, B_e) were calculated for the $X\,^2\Sigma^+$ and $A\,^2\Pi$ states of the MH species. The comparison between our present work and available theoretical and experimental results in literature

shows a good agreement. We also studied and compared the spectroscopic constants with and without spin-orbit interactions included in electronic structure calculations of CaH, SrH, and BaH at MRCI level. These results suggest that the effect of spin-orbit coupling on the spectroscopic parameters with all-electron calculations did not show a significant impact with respect to the results of the spin-free relativistic ECP-MRCI approach.

Using the PECs and TDMs obtained, we have shown a full scene of the highly diagonally distributed FCFs $f_{v'v}$ for transitions between the $A\,^2\Pi(v') \rightarrow X\,^2\Sigma^+(v)$ of the MH species. At the same time, we also determined the radiative lifetime and radiative width for the first six vibrational levels ($v' = 0 - 5$) of $A\,^2\Pi$ states of MH species. The computed short lifetimes are sufficient to produce larger spontaneous scattering forces. These results suggest a scheme for a viable laser cooling cycle for MH species. The FCFs, radiative lifetimes, radiative width, and wavelength $\lambda_{vv'}$ between $A\,^2\Pi_{1/2,3/2}(v')$ and $X\,^2\Sigma_{1/2}(v)$ states of CaH, SrH, and BaH can be found in the Supplemental Material [67].

[1] E. S. Shuman, J. F. Barry, D. R. Glenn, and D. DeMille, Phys. Rev. Lett. **103**, 223001 (2009).
[2] E. S. Shuman, J. F. Barry, and D. DeMille, Nature (London) **467**, 820 (2010).
[3] J. F. Barry, E. S. Shuman, E. B. Norrgard, and D. DeMille, Phys. Rev. Lett. **108**, 103002 (2012).
[4] M. T. Hummon, M. Yeo, B. K. Stuhl, A. L. Collopy, Y. Xia, and J. Ye, Phys. Rev. Lett. **110**, 143001 (2013).
[5] V. Zhelyazkova, A. Cournol, T. E. Wall, A. Matsushima, J. J. Hudson, E. A. Hinds, M. R. Tarbutt, and B. E. Sauer, Phys. Rev. A **89**, 053416 (2014).
[6] L. D. Carr, D. DeMille, R. V. Krems, and J. Ye, New J. Phys. **11**, 055049 (2009).
[7] M. D. Di Rosa, Eur. Phys. J. D **31**, 395 (2004).
[8] T. A. Isaev, S. Hoekstra, and R. Berger, Phys. Rev. A **82**, 052521 (2010).
[9] N. Wells and I. C. Lane, Phys. Chem. Chem. Phys. **13**, 19018 (2011).
[10] I. C. Lane, Phys. Chem. Chem. Phys. **14**, 15078 (2012).
[11] B. Yadin, T. Veness, P. Conti, C. Hill, S. N. Yurchenko, and J. Tennyson, Mon. Not. R. Astron. Soc. **425**, 34 (2012).
[12] R. Celiberto, K. L. Baluja, and R. K. Janev, Plasma Sources Sci. Technol. **22**, 015008 (2013).
[13] M. Mostafanejad and A. Shayesteh, Chem. Phys. Lett. **551**, 13 (2012).
[14] E. GharibNezhad, A. Shayesteh, and P. F. Bernath, Mon. Not. R. Astron. Soc. **432**, 2043 (2013).
[15] R. D. E. Henderson, A. Shayesteh, J. Tao, C. C. Haugen, P. F. Bernath, and R. J. Le Roy, J. Phys. Chem. A **117**, 13373 (2013).
[16] K. H. Hinkle, L. Wallace, R. S. Ram, P. F. Bernath, C. Sneden, and S. Lucatello, Astrophys. J., Suppl. Ser. **207**, 26 (2013).
[17] R. H. Zhang and T. C. Steimle, Astrophys. J. **781**, 51 (2014).
[18] T. C. Steimle, R. H. Zhang, and H. Wang, J. Chem. Phys. **140**, 224308 (2014).
[19] G. Li, J. J. Harrison, R. S. Ram, C. M. Western, and P. F. Bernath, J Quant. Spectrosc. Radiat. Transfer **113**, 67 (2012).
[20] E. GharibNezhad, A. Shayesteh, and P. F. Bernath, J. Mol. Spectrosc. **281**, 47 (2012).
[21] A. Shayesteh, R. S. Ram, and P. F. Bernath, J. Mol. Spectrosc. **288**, 46 (2013).
[22] T. Leininger and G. H. Jeung, Phys. Rev. A **49**, 2415 (1994).
[23] P. S. Ramchandran, N. Rajamanickam, and S. P. Bagare, Serb. Astron. J. **172**, 13 (2006).
[24] L.-E. Berg, K. Ekvall, A. Hishikawa, S. Kelly, and C. Mcguinness, Chem. Phys. Lett. **255**, 419 (1996).
[25] T. Pauchard, M. Liu, O. Launila, and L.-E. Berg, J. Mol. Spectrosc. **247**, 181 (2008).
[26] A. Shayesteh, K. A. Walker, I. Gordon, D. R. T. Appadoo, and P. F. Bernath, J. Mol. Struct. **695-696**, 23 (2004).
[27] R. S. Ram, K. Tereszchuk, K. A. Walker, and P. F. Bernath, J. Mol. Spectrosc. **271**, 15 (2012).
[28] P. Fuentealba, O. Reyes, H. Stoll, and H. Preuss, J. Chem. Phys. **87**, 5338 (1987).
[29] P. Fuentealba and O. Reyes, Mol. Phys. **62**, 1291 (1987).
[30] M. Kaupp, P. v. R. Schleyer, H. Stoll, and H. Preuss, J. Chem. Phys. **94**, 1360 (1991).
[31] A. R. Allouche, G. Nicolas, J. C. Barthelat, and F. Spiegelmann, J. Chem. Phys. **96**, 7646 (1992).
[32] M. Aymar and O. Dulieu, J. Phys. B: At. Mol. Opt. Phys. **45**, 215103 (2012).
[33] L.-E. Berg, K. Ekvall, A. Hishikawa, and S. Kelly, Phys. Scripta **55**, 269 (1997).
[34] U. Magg, H. Birk, and H. Jones, Chem. Phys. Lett. **149**, 321 (1988).
[35] K. A. Walker, H. G. Hedderich, and P. F. Bernath, Mol. Phys. **78**, 577 (1993).
[36] R. S. Ram and P. F. Bernath, J. Mol. Spectrosc. **283**, 18 (2013).
[37] H.-J. Werner and P. J. Knowles, J. Chem. Phys. **82**, 5053 (1985).
[38] P. J. Knowles and H.-J. Werner, Chem. Phys. Lett. **115**, 259 (1985).
[39] H.-J. Werner and P. J. Knowles, J. Chem. Phys. **89**, 5803 (1988).
[40] P. J. Knowles and H.-J. Werner, Chem. Phys. Lett. **145**, 514 (1988).
[41] S. R. Laughoff and E. R. Davidson, Int. J. Quantum Chem. **8**, 61 (1974).
[42] N. Douglas and N. M. Kroll, Ann. Phys. **82**, 89 (1974).
[43] B. A. Hess, Phys. Rev. A **33**, 3742 (1986).
[44] H.-J. Werner, P. J. Knowles, R. Lindh, F. R. Manby, M. Schütz, P. Celani, T. Korona, R. Lindh, A. Mitrushenkov, G. Rauhut, K. R. Shamasundar, T. B. Adler, R. D. Amos, A. Bernhardsson, A. Berning, D. L. Cooper, M. J. O. Deegan, A. J. Dobbyn, F. Eckert, E. Goll *et al.*, MOLPRO is a package of *ab initio* programs, version 2009.1 (see http://www.molpro.net).
[45] D. Feller, J. Comput. Chem. **17**, 1571 (1996).
[46] K. L. Schuchardt, B. T. Didier, T. Elsethagen, L. Sun, V. Gurumoorthi, J. Chase, J. Li, and T. L. Windus, J. Chem. Inf. Model. **47**, 1045 (2007).
[47] T. H. Dunning Jr., J. Chem. Phys. **90**, 1007 (1989).
[48] I. S. Lim, H. Stoll, and P. Schwerdtfeger, J. Chem. Phys. **124**, 034107 (2006).

[49] A. Berning, M. Schweizer, H.-J. Werner, P. J. Knowles, and P. Palmieri, Mol. Phys. **98**, 1823 (2000).
[50] M. A. Iron, M. Oren, and J. M. L. Martin, Mol. Phys. **101**, 1345 (2003).
[51] C. L. Barros, P. J. P. de Oliveira, F. E. Jorge, A. Canal Neto, and M. Campos, Mol. Phys. **108**, 1965 (2010).
[52] R. J. Le Roy, *LEVEL 8.0, A Computer Program for Solving the Radial Schrödinger Equation for Bound and Quasibound Levels*, Chemical Physics Research Report 663 (University of Waterloo, Waterloo, ON, 2007).
[53] C. Henriet and G. Verhaegen, Phys. Scr. **33**, 299 (1986).
[54] J. Pitarch-Ruiz, J. Sánchez-Marin, A. M. Velasco, and I. Martin, J. Chem. Phys. **129**, 054310 (2008).
[55] *NIST Chemistry WebBook, NIST Standard Reference Database Number 69*, edited byP. J. Linstrom and W. G. Mallard (National Institute of Standards and Technology, Gaithersburg, MD, 2005). Available at http://webbook.nist.gov.
[56] M. Guitou, A. Spielfiedel, and N. Feautrier, Chem. Phys. Lett. **488**, 145 (2010).
[57] A. Shayesteh, D. R. T. Appadoo, I. Gordon, R. J. Le Roy, and P. F. Bernath, J. Chem. Phys. **120**, 10002 (2004).
[58] A. Shayesteh, R. D. E. Henderson, R. J. Le Roy, and P. F. Bernath, J. Phys. Chem. A **111**, 12495 (2007).
[59] A. Shayesteh and P. F. Bernath, J. Chem. Phys. **135**, 094308 (2011).
[60] J.-M. Mestdagh, P. de Pujo, B. Soepa, and F. Spiegelmanb, Chem. Phys. Lett. **471**, 22 (2009).
[61] T. Leininger and G. Jeung, J. Chem. Phys. **103**, 3942 (1995).
[62] M. Korek, H. Razzouk, R. A. Arkoub, and S. E. Atwani, Adv. Mater. Res. **324**, 282 (2011).
[63] O. Appelblad, L. Klynning, and J. W. C. Johns, Phys. Scr. **33**, 415 (1986).
[64] A. Benrnard, C. Effantin, J. D'Incan, G. Fabre, R. Stringat, and R. F. Barrow, Mol. Phys. **67**, 1 (1989).
[65] C. Focsa, S. Firth, P. F. Bernath, and R. Colin, J. Chem. Phys. **109**, 5795 (1998).
[66] L.-E. Berg and L. Klynning, Phys. Scr. **10**, 331 (1974).
[67] See Supplemental Material at http://link.aps.org/supplemental/10.1103/PhysRevA.90.052506 for FCFs, radiative lifetimes, radiative width, and wavelength $\lambda_{vv'}$ between $A\,^2\Pi_{1/2,3/2}(v')$ and $X\,^2\Sigma_{1/2}(v)$ states of CaH, SrH, and BaH.
[68] F. B. C. Machado, O. Roberto-Neto, and F. R. Ornellas, Chem. Phys. Lett. **305**, 156 (1999).
[69] O. Nedelec and J. Dufayard, J. Chem. Phys. **69**, 1833 (1978).
[70] M. Liu, T. Pauchard, M. Sjödin, O. Launila, P. van der Meulen, and L.-E. Berg, J. Mol. Spectrosc. **257**, 105 (2009).